

# Fiber Bragg gratings for stress field characterization inside a connector

Linda K. Baker<sup>a</sup>, Vikram Bhatia<sup>a</sup>, G. Scott Glaesemann<sup>a</sup>, Marlene A. Marro<sup>a</sup>, Charles Mansfield<sup>b</sup>

<sup>a</sup>Corning Incorporated, Corning, NY 14831

<sup>b</sup>3M, Telecom Systems Division, 3M Austin Center, Austin, TX 78726

## ABSTRACT

This study presents results from an experiment where Bragg gratings were used to measure the stress on a bare optical fiber placed inside a 3M VF-45 connector. The connector exerts lateral compressive and longitudinal tensile stresses on the fiber, both of which yield a shift in the Bragg wavelength. The axial stress is of interest for mechanical reliability predictions, so additional measurements were performed in order to separate the two effects. This involved simulating the use of an alternate material in the connector to induce differential longitudinal stress on the fiber grating.

**Keywords:** Bragg grating, reliability, transverse strain, VF-45 connector

## 1. INTRODUCTION

The evolution of small form factor connectors for glass optical fiber has resulted in connector designs that place optical fiber in new configurations. The mechanical reliability of fiber in connectors is of particular importance and has been the subject of previous investigations.<sup>1</sup> The reliability assessment requires knowledge of applied stresses on the fiber inside the connector. The purpose of this paper is to describe the use of fiber Bragg gratings for experimentally determining applied axial stress in a new connector design, the ferrule-less VF-45<sup>TM</sup> connector from 3M.

## 2. THE VF-45<sup>TM</sup> CONNECTOR

Bare optical fiber is secured in the field-terminated wall socket by crimping it in a soft aluminum element. A schematic of the VF-45 wall socket fiber holder is shown in Figure 1. The transition from coated to bare fiber occurs approximately mid-way through the aluminum crimping element. The aluminum element has a pre-made groove fabricated into it, as shown in Figure 2. The aluminum metal is soft, and purposefully deforms around the fiber when crimped, exerting a diametric compression load on the optical fiber as well as a tensile load as it plastically deforms.

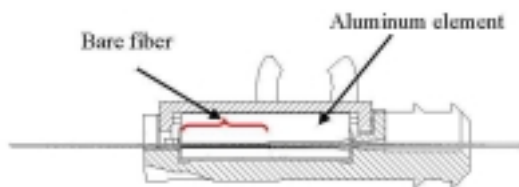


Figure 1. Schematic of VF-45 wall socket fiber holder.

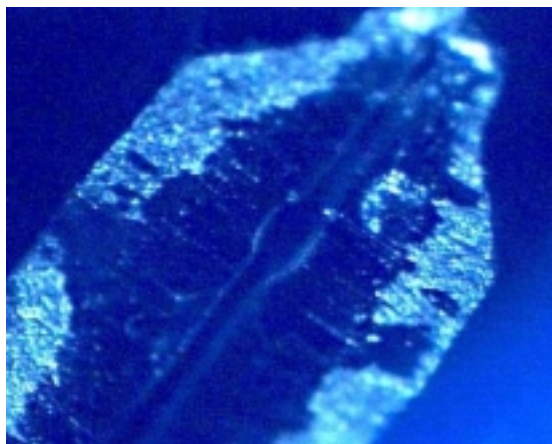


Figure 2. End-view of aluminum crimping element found inside VF-45 wall socket.

### 3. EXPERIMENT

For this work, two sets of fiber Bragg grating laboratory measurements were collected. A broadband ASE source centered at 1550 nm was used in the experimental set-up. Reflected light from the grating was recovered using a 3-port optical circulator. The reflected spectra were displayed on an Optical Spectrum Analyzer (OSA). As the grating was strained a blue shift in the center wavelength was observed and recorded as a function of the applied strain. The measurement collection schematic is shown in Figure 3.

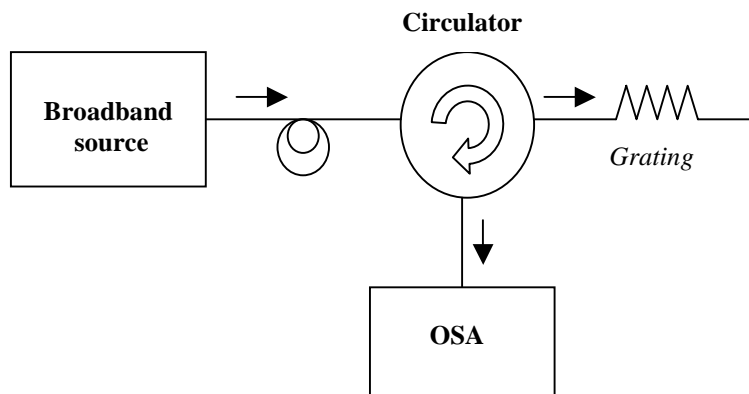


Figure 3. Schematic of measurement collection setup.

#### A. Wall socket measurements

Corning high delta fiber with Bragg gratings (> 40 mm long, 3 dB BW Rx < 0.5 nm) were inserted into the VF-45 wall socket fiber holder, and the aluminum element was crimped around the fiber. A reflection measurement was collected both before and after securing the fiber in the fiber holder. A total of three measurements were collected, averaging a 1.490 nm wavelength shift. The individual data points are given in Table I. Representative spectrums are shown in Figure 4. 3M estimates that the fiber holder exerts a 20 lb (89 N) diametric compression force on the optical fiber once it has been secured.<sup>2</sup>

Table I. Measurements collected in VF-45 wall socket.

	Starting Wavelength (nm)	Final Wavelength (nm)	Wavelength Shift (nm)
Grating #1	1534.154	1535.673	1.519
Grating #2	1553.241	1554.736	1.495
Grating #3	1555.961	1557.418	1.457

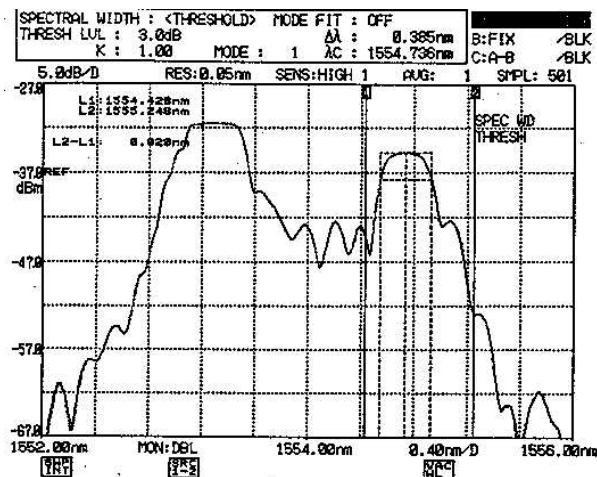
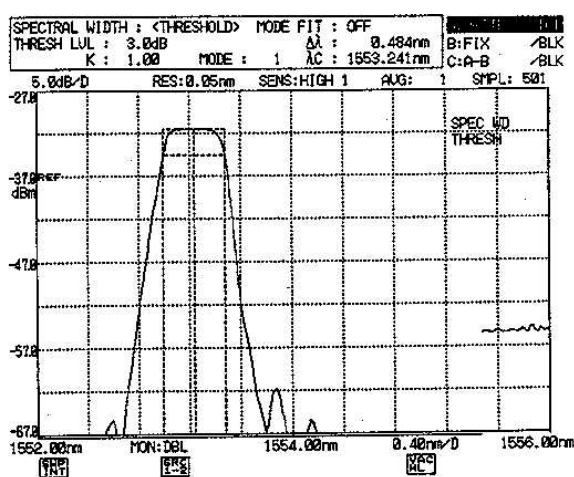


Figure 4. Reflection spectrum from grating #2: (a) Initial measurement before securing fiber in element, and (b) after crimping element around fiber.

*B. Measurements with different materials*

The center wavelength shifts reported in Table I are the combined effect of the diametric compression and the plastic deformation of the soft aluminum. The aluminum deforms in the direction of the free ends of the crimp region, and therefore, places some axial tensile strain on the fiber. From a mechanical reliability point of view, only the axial strain is of interest. In order to determine the amount of wavelength shift due solely to the axial strain, we needed to quantify the transverse loading effect. We did this in a laboratory test setup by diametrically loading the fiber between steel plates, which deforms much less than the soft aluminum metal under the same loading conditions. In this setup, the fiber experiences similar transverse loading strains but not the additional axial strain. The test configuration is shown in Figure 5 below. The measurements were performed with both aluminum and steel blocks; the 1.600 nm wavelength shift measured with the aluminum blocks prove consistency between the experimental setup described and the actual VF-45 wall socket where an average wavelength shift of 1.490 nm was found.

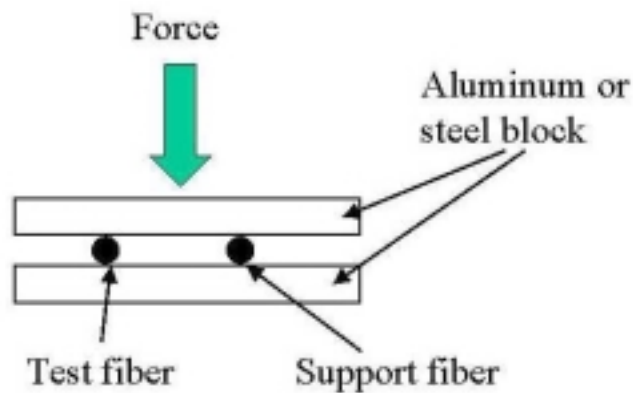


Figure 5. Mechanical configuration for application of diametric loads to fiber Bragg grating.

In this case, a Bragg grating of approximately 0.1mm in length (3 dB BW Rx > 3nm) in a CS 980 fiber was used. The results of these measurements are shown in Figure 6, with the individual data points given in Table II. The same fiber Bragg grating was used for both measurements.

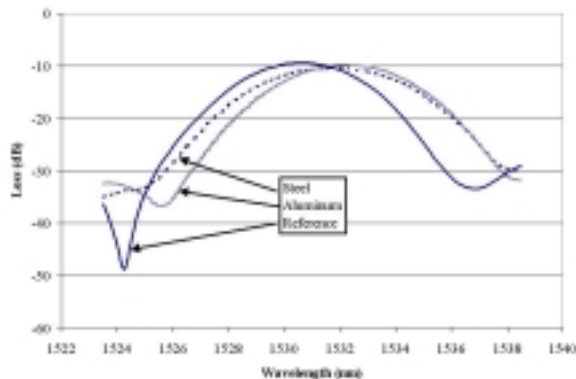


Table II.

Material	Starting Wavelength (nm)	Final Wavelength (nm)	Wavelength Shift (nm)
Aluminum	1530.627	1532.227	1.600
Steel	1530.630	1531.770	1.140

Figure 6. Reflected spectra collected in laboratory configuration. The reference line is the initial spectrum before any load is applied.

With no load applied, the reflected spectrum has a single peak centered around the nominal Bragg wavelength of 1530 nm. When a 20 lb (89 N) load is applied to the Bragg grating, we see a broadening of the reflected spectrum and an increase in the Bragg grating wavelength. There is more broadening in the spectrum when clamped between two steel plates rather than when between softer aluminum plates.

#### 4. ANALYSIS

The experimental measurements can be compared to the expected theoretical results for fiber under diametric loading. As has been shown previously,<sup>3</sup> purely diametric loads on a circular fiber results in plane strain ( $\epsilon_{zz} = 0$ ) creating the stress state given below:

$$\sigma_{xx} = \frac{2F}{\pi h D} \quad \text{and} \quad \sigma_{yy} = -\frac{6F}{\pi h D} \quad (1)$$

where  $D$  is the diameter of the fiber (125  $\mu\text{m}$ ), and the thickness  $h$  is the length of the fiber under loading (0.5 cm). Once the stresses have been calculated, the values of the strain state can be found from Hooke's law for plane strain:

$$\epsilon_{xx} = \frac{1+\nu}{E} [\sigma_{xx}(1-\nu) - \nu\sigma_{yy}] \quad \text{and} \quad \epsilon_{yy} = \frac{1+\nu}{E} [\sigma_{yy}(1-\nu) - \nu\sigma_{xx}] \quad (2)$$

where  $E$  is Young's modulus (70.3 GPa), and  $\nu = 0.19$  is Poisson's ratio. From this, the wavelength shift is calculated by:

$$\frac{\Delta\lambda_x}{\lambda_x} = -\frac{1}{2}n_o^2 [P_{11}\epsilon_{xx} + P_{12}\epsilon_{yy}] \quad \text{and} \quad \frac{\Delta\lambda_y}{\lambda_y} = -\frac{1}{2}n_o^2 [P_{11}\epsilon_{yy} + P_{12}\epsilon_{xx}] \quad (3)$$

Here  $n_o = 1.45$  is the average index of refraction, and the respective strain-optic coefficients  $P_{11}$  and  $P_{12}$  are 0.113 and 0.252.<sup>4</sup> Using these equations, we find that the predicted average wavelength shift ( $\Delta\lambda_x + \Delta\lambda_y$ ) for a Bragg grating under a 20 lb (89 N) load is 1.12 nm.

There is good agreement between the calculated wavelength shift of 1.12 nm and the experimental results obtained with the steel plates in the experimental setup (1.14 nm). This further indicates that only the transverse strain effect is occurring in the steel plate experiment. The wavelength shift differential between the steel and aluminum plates (1.60 – 1.14 = 0.46 nm) is therefore due solely to the amount of additional axial stress caused by the soft aluminum deforming as the load is applied, and axially stretching the fiber. The axial strain in the fiber can be estimated using equation (4) below,<sup>5</sup> and then converted to a stress using Hooke's law, equation (5). The axial stress in the fiber after being crimped in the VF-45 wall socket fiber holder is calculated to be 3.8 kpsi (0.026 GPa).

$$\frac{\Delta\lambda}{\lambda_o} = \left\{ 1 - \frac{1}{2}n_o^2 [P_{12} - \nu(P_{11} + P_{12})] \right\} \epsilon \quad (4)$$

$$\sigma = E\epsilon \quad (5)$$

In order to verify the amount of axial stress in the optical fiber after being crimped in the VF-45 wall socket, 3M performed a finite element analysis (FEA)<sup>6</sup> whose results are shown in Figure 7 below. It was estimated that the stress in the core of the fiber was 5-7 kpsi. Overall, there is reasonable agreement between the 3.8 kpsi of axial stress determined experimentally and the 5-7 kpsi estimated from the 3M FEA.

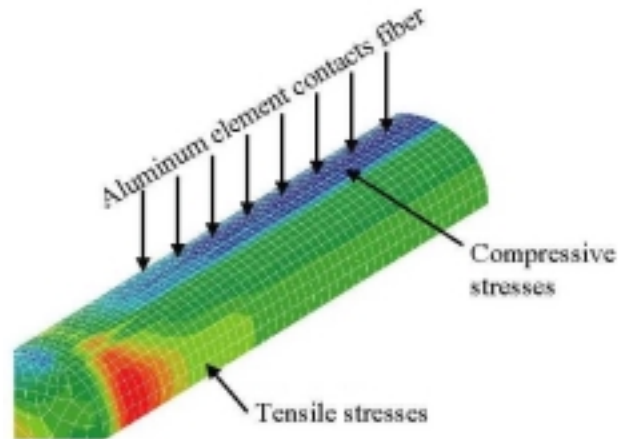


Figure 7. FEA model of stress on fiber inside wall socket fiber holder. Provided by 3M.

## 5. CONCLUSIONS

Fiber Bragg gratings were used to experimentally determine the amount of axial stress on optical fiber inside the 3M VF-45 wall socket. The differential between the Bragg grating wavelength shift measured when the fiber was loaded between hard steel and soft aluminum plates was indicative of the axial stress induced during the deformation of the aluminum metal. The experimentally determined value of 3.8 kpsi agreed well with FEA results of 5-7 kpsi supplied by 3M. In addition, the measured wavelength shift due to the transverse stress created during the diametric loading condition agreed well with the predicted wavelength shift. This study shows that Bragg gratings can be used as a stress measurement tool when estimating lifetimes for fibers in connectors.

## ACKNOWLEDGEMENTS

The authors would like to thank Vern Radewald of 3M for performing the VF-45 FEA work, and Jim Sirkis of the University of Maryland for providing valuable insight and advice.

## REFERENCES

1. W.R. Wagner, "Failure Analysis of Fiber Optic Connectors," *Advances in Ceramics, Volume 22, Fractography of Glasses and Ceramics*, 389-402, American Ceramic Society (1988).
2. Correspondence with C. Mansfield, 3M, Telecom Systems Division, Austin, TX.
3. R.B. Wagreich, W.A. Atia, H. Singh, and J.S. Sirkis, "Effects of diametric load on fibre Bragg gratings fabricated in low birefringent fibre", *Electronic Letters* (1996) **32**, 13, pp. 1223-1224.
4. A. Bertholds and R. Dandliker, "Determination of the Individual Strain-Optic Coefficients in Single-Mode Optical Fibers", *J. Lightwave Technology* (1988) **6**, 1, pp. 17-20.
5. A.T. Alavie et al, "Characteristics of fiber grating sensors and their relation to manufacturing techniques", *SPIE Vol. 2444*, pp. 528-535.
6. Correspondence with C. Mansfield, 3M, Telecom Systems Division, Austin, TX.